JOURNAL OF OPTOELECTRONICS AND ADVANCED MATERIALS Vol. 10, No 10, October 2008, p. 2599 - 2602

Electrical and optical properties of nanostructured ZnO thin films for optoelectronic applications

L. ION[a], M. I. RUSU[b], G. SOCOL[c], I. N. MIHĂILESCU[c], C. TĂZLĂOANU[a], S. ANTOHE[a*]
[a] *University of Bucharest, Faculty of Physics, RO-077125 Măgurele-Ilfov, POB MG-11, Romania*
[b] *National Institute for Research and Development for Optoelectronics, INOE 2000, 1 Atomistilor Street, Magurele, Romania*
[c] *National Institute for Plasma Physics, RO-077125 Măgurele-Ilfov, Romania*

Electrical and optical characterization of ZnO thin films produced by pulsed laser deposition (PLD) have been carried out. The films were deposited under various conditions and were optimized for use in hybrid organic/inorganic photovoltaic cells. XRD spectra revealed they had a polycrystalline structure of wurtzite type, preferentially oriented along the [001] axis situated in the growth direction. With increasing substrate temperature, the texture improves. The electrical properties of the films were studied over a large temperature range. Charge transport occurs through either a conduction band mechanism, at high temperatures, and hopping at temperatures below 60 K. The main defects controlling electrical properties of the films were investigated by the method of thermally stimulated currents.

(Received August 5, 2008; accepted August 28, 2008).

Keywords: Zinc oxide, PLD, XRD, TSC, Optical properties

1. Introduction

Wurtzite-type ZnO is a direct band-gap semiconductor with optical properties recommending it as a good candidate for optoelectronic applications. Its wide band-gap energy, a large absorption coefficient and a very large exciton binding energy (60 meV) [1], are particularly interesting for the fabrication of optoelectronic devices operating in the blue and UV region of the spectrum. Considerable research efforts were focused in the last decade on the study of ZnO [2-7], aiming at understanding various physical properties (the origin of n-type conduction and of some luminescence lines, effects of doping with magnetic impurities, etc.).

Several techniques for producing good quality ZnO crystals or films were proposed. Among them, pulsed laser deposition (PLD) was proved to be the best one for preserving the target compositions. PLD is recognized as a versatile technique for producing thin solid films with complex chemical compositions and various properties and morphological characteristics.

In this paper we report on the electrical and optical properties of ZnO thin films deposited by PLD and optimized for use in hybrid organic/inorganic photovoltaic cells. Electrical properties of the films were studied over a large temperature range (30 K – 300 K). The main defects controlling electrical properties of the films were investigated by thermally stimulated current (TSC) method, largely used for this purpose [8-16]. Optical absorption spectra were also recorded and discussed. The influence of deposition parameters on the films properties was investigated.

2. Experimental

ZnO thin films were deposited by PLD (KrF* $\lambda = 248$ nm and $\tau_{FWHM} \approx 7$ ns) on optical glass substrates and optical glass coated with 30 nm - thick ITO films. The reaction chamber was evacuated down to a residual gas pressure below 10^{-4} Pa. Data regarding the preparation conditions of the films analyzed in this study are shown in Table 1.

Table 1. PLD deposition parameters.

Sample	Target	Substrate	Deposition temperature [º C]	Oxygen pressure [Pa]
ZOC	ZnO	Optical glass	RT	13.3
ZOC2	ZnO	Optical glass	RT	133
ZSC1	ZnO	30 nm ITO coated optical glass	RT	13
ZSC3	ZnO	30 nm ITO coated optical glass	200	13
ZSC5	ZnO	30 nm ITO coated optical glass	200	6.5
ZSC7	ZnO	30 nm ITO coated optical glass	200	40
ZSC9	ZnO	30 nm ITO coated optical glass	350	13

Electrical measurements were performed using a Keithley 2400 Source Meter and a Keithley 6517 electrometer. The films were placed in a He closed cycle cryostat with sample in vacuum (residual pressure was below 10^{-2} Pa), having four quartz windows for optical access to the sample. The temperature of the analyzed

samples was varied between 20 K and 300 K. The resistance was measured in a four-point configuration.

Thermally stimulated current (TSC) analysis was performed after filling the traps by adequate illumination (395 nm light, for 15 min.) at 40 K. The constant heating rate was 0.1 K/s.

3. Results

Structural analysis of the samples by X-ray diffraction revealed that the films consist of a hexagonal-close-packed wurtzite type phase ZnO, preferentially oriented along [001] axis in the growth direction [16].

It was observed that on increasing the oxygen pressure during deposition, the film texture got more pronounced.

3.1 Electrical properties

The measured electrical resistance, in logarithmic scale against the reciprocal of temperature, is shown in Fig. 1. In some limited temperature ranges, *R(T)* dependence is well described by:

$$R(T) = R_o(T)\exp\left(\frac{E_a}{k_B T}\right) \qquad (1)$$

where E_a is the activation energy. The pre-exponential factor R_o may have a slight temperature dependence, reflecting the temperature dependence of free carriers. Both E_a and R_0 parameters, as obtained by numerical fit in the indicated temperature ranges are presented in Table 2. At room temperature and down to 180 K – 230 K, the experimental results suggest a band conduction mechanism, controlled by different donor centers. The sample indexed ZSC9 has the largest conductivity, due to a shallow donor located at 0.031 eV below the bottom edge of the conduction band. Note also the constant activation energy (0.056 eV) existing in a rather limited temperature range (100 K – 140 K) in the case of ZOC2 sample, which has main donor centers with ionization energy of E_1=0.139 eV. This can be explained as due to the hopping of the charge carriers over some compensated donor states, located at 0.056 eV above the main donor (E_2=0.083 eV below the bottom edge of the conduction band). The number of hopping electrons, n_h, is exponentially small $\left(n_h \propto e^{-\frac{E_1-E_2}{k_B T}}\right)$, but their mobility is larger, due to a larger localization radius of E_2 state. For that reason the above-mentioned mechanism could become dominant in a finite temperature range.

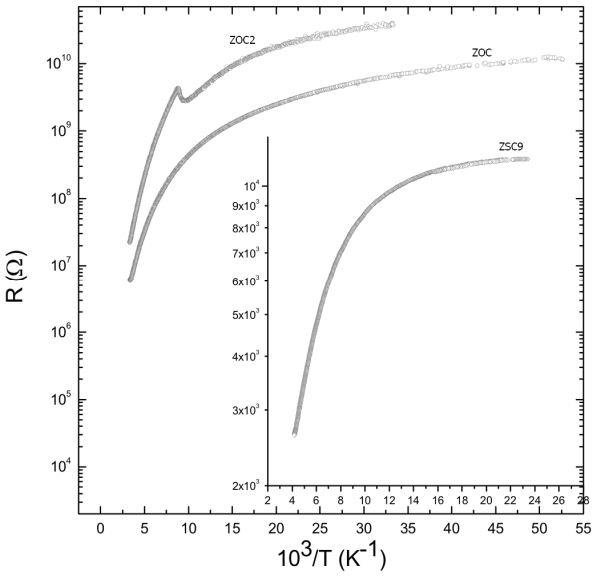

Fig. 1. Temperature dependence of the electrical resistance of the films.

Table 2. Parameters characterizing the electrical resistance (eq. (1)), as obtained by numerical fit.

Temperature range [K]	E_a [eV]	R_0 [Ω]	Sample.
300-200	0.10	1.11×10^5	ZOC
40-20	3×10^{-3}	2.065×10^9	ZOC
300-230	0.139	1.34×10^5	ZOC2
140-110	0.056	1.51×10^7	ZOC2
40-20	4.5×10^{-3}	7.089×10^9	ZOC2
250-180	0.03	633.46	ZSC9

In the low temperature range, E_a and R_o values can be explained assuming that the electrical conduction comes from electrons hopping between the main donor states, partially emptied by compensation.

Thermally stimulated current spectra are shown in Fig. 2. A well resolved TSC peak, originating from thermal release of charge carriers from a trap having activation energy E_{t0} into conduction or valence band, is described by [11]:

$$I_{TSC}(T) = I_o \exp\left(-\int_{T_0}^{T}\frac{e_t}{\beta}dT'\right), \qquad (2)$$

where $I_o = Ce\mu\tau N_t e_t V$, e is the electron charge, μ and τ are, respectively, the mobility and lifetime of free carriers, V is the applied voltage, C is a geometrical factor (for a sample having the length l, width w and thickness d, $C=wd/l$), N_t is the traps density, T_o is the starting temperature, β is the heating rate and e_t is the emission rate from the trap, given by:

$$e_t = \frac{16\pi m^* k_B^2}{h^3}\sigma_t T^2 \exp\left(-\frac{E_{t0}}{k_B T}\right). \quad (3)$$

In eq. (3) m^* is the free carriers effective mass, h is Planck's constant, k_B is Boltzmann's constant, σ_t is the free carriers capture cross-section and E_{t0} is the ionization energy of the traps. Usually, the temperature dependence of σ_t can be expressed as $\sigma_t = \sigma_{t0}\exp\left(-E_\sigma / k_B T\right)$ and the experimentally measured trap activation energy is then $E_t = E_{t0} + E_\sigma$.

In the stage of initial raise of a TSC peak, the integral in eq. (2) is negligible, and the temperature dependence of the thermally stimulated current is given by:

$$I_{TSC}(T) \propto \exp\left(-\frac{E_t}{k_B T}\right). \quad (4)$$

Using eq. (4), the activation energy of the traps can be easily determinated, if the peaks are well separated. In the case of the sample indexed ZOC2 (Fig. 2a), the ionization energy of the traps contributing to the main peak, as determined experimentally, is E_t=0.141 eV, and the density of traps, extracted from the peak area is $N_t = 1.18\times10^{22}$ m^{-3}. Comparing with values in table II, one can conclude that these traps represent the main donors controlling the electrical properties of the sample.

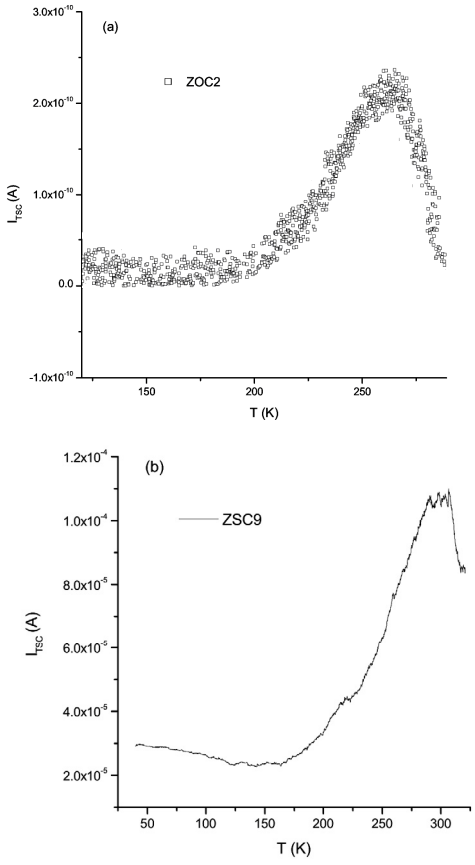

Fig. 3. TSC spectra recorded for the samples ZOC2 (a) and ZSC9 (b).

In the case of ZSC9 sample, the TSC spectrum (Fig. 2b), suggests the presence of several trapping levels. The peak, centered at 300 K, is too large to be associated to a single trap. A shoulder is observed at 220 K.

3.3 Optical properties

Fig. 3 shows the absorption spectra recorded for the samples indexed ZSC1-7. A bump, at 3.04 – 3.11 eV can be observed, more pronounced in the case of ZSC5 sample. It may be associated to a acceptor center – conduction band transition. Note that the oxygen pressure during the deposition of ZSC5 sample was the lowest (Table 1), which suggests that the above-mentioned center could be associated to an oxygen vacancy or to a complex defect involving an oxygen vacancy. For the samples deposited at lower substrate temperatures, the bump broadens toward lower photon energies, which may be explained by the fact that the substrate temperature was insufficient for getting films of high quality. This is also supported by the XRD data.

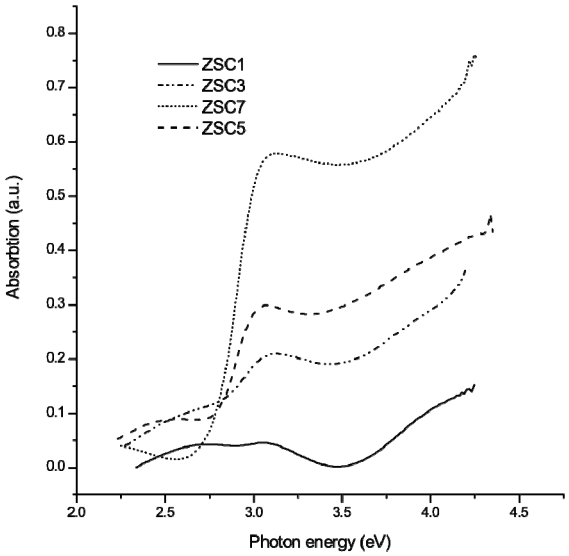

Fig. 3. Optical absorption spectra of analyzed samples.

3. Conclusions

Electrical and optical characterizations of PLD deposited ZnO thin films were performed. There was observed that the structural quality of the films improves with increasing the substrate temperature and the oxygen pressure during deposition. Several donor centers, controlling the electrical properties of the films, were detected, their presence depending strongly on the growth conditions. With larger substrate temperatures and lower oxygen pressure, the samples become more conductive. For all analyzed samples, a bump is observed in the optical absorption spectra, at photon energies of 3.04 eV – 3.11 eV, corresponding to a band – localized center

transition. It broadens towards lower photon energies with decreasing the substrate temperature during deposition.

Acknowledgement

This work was financially supported by the Romanian Ministry of Education and Research, under Ceex06 Program, Grants No. 29/2006 and 53/2006

References

[1] W. Y. Liang, A. D. Yoffe, Phys. Rev. Lett. **20**, 59 (1968).
[2] P. Sati, R. Hayn, R. Kuzian, S. Regnier, S. Schafer, A. Stepanov, C. Morhain, C. Deparis, M. Laugt, M. Goiran, and Z. Golacki, Phys. Rev. Lett. **96**, 17203 (2006).
[3] R. Yakimova, G.R. Yazdi, N.T. Son, I. Ivanov, M. Syvjrvi, S. Sun, G. Tompa, A. Kuznetsov , B. Svensson, Superlatt. Microstruct. **39**, 247 (2006).
[4] L. E. Halliburton, N.C. Giles, N.Y. Garces, Ming Luo, Chunchuan Xu, Lihai Bai, and L.A. Boatner, Appl. Phys. Lett. **87**, 172108 (2005).
[5] L. S. Vlasenko, G. D. Watkins, R. Helbig, Phys. Rev. **B71**,115205 (2005).
[6] Ya. I. Alivov, M. V. Chukichev, V. A. Nikitenko, Semiconductors **38**, 31 (2004).
[7] D. Li, Y.H. Leung, A.B. Djurisic, Z.T. Liu, M.H. Xie, S.L. Shi, S.J. Xu, and W.K. Chan, Appl. Phys. Lett. **85**, 1601 (2004).
[8] G. F. J. Garlick, A. F. Gibson, Proc. Phys. Soc. London **60**, 574 (1948).
[9] M. Pavlovič, U. V. Desnica, J. Appl. Phys. **84**, 2018 (1998).
[10] Z-Q. Fang, D. C. Look, Appl. Phys. Lett. **59**, 48 (1991).
[11] D. C. Look, in: R. K. Willardson and A. C. Beer (Eds.), Semiconductors and Semimetals, vol. 19, Academic Press, New York, 1983, p. 75.
[12] R. Fasbender, G. Hirt, M. Thoms, A. Winnacker, Semicond. Sci. Technol. **11**, 935 (1996).
[13] L. Ion, S. Antohe , M. Popescu, F. Scarlat, F. Sava, Felicia Ionescu, J. Optoelectron. Adv. Mater. **6**(1), 113 (2004),
[14] L. Ion, S. Antohe, J. Appl. Phys. **97**(1), 3513 (2005).
[15] S. Antohe, L. Ion, V. A. Antohe, M. Ghenescu, H. Alexandru, J. Optoelectron. Adv. Mater., **9**(5), 1382 (2007).
[16] C. Tazlaoanu, L. Ion, G. Socol, Marcela Socol, I. N. Mihailescu, F. Stanculescu, I. Enculescu, Felicia Ionescu, Oana Ghenescu, Larisa Magheruşan, S. Antohe, J. Optoelectron. Adv. Mater. **9**(5), 1342 (2007).

*Corresponding author : lucian@solid.fizica.unibuc.ro